Modelling Frequency Variations in Power System Models for Transient Stability Analysis

Prof. Federico Milano

Email: federico.milano@ucd.ie

Webpage: faraday1.ucd.ie

School of Electrical & Electronic Engineering

University College Dublin

Dublin, Ireland

Biography

- Federico Milano received from the University of Genoa, Italy, the Electrical Engineering degree and the Ph.D. degree in 1999 and 2003, respectively.
- In 2001 and 2002, he worked at the University of Waterloo, Canada, as a Visiting Scholar.
- From 2003 to 2013, he was with University of Castilla-La Mancha, Ciudad Real, Spain.
- He joined University College Dublin, Ireland, in 2013, where he is currently Professor in Power Systems Control and Protections.
- In January 2016, he was elevated to *IEEE Fellow* for his contributions to power systems modelling ans simulation.

Contents

- Motivations
- Existing methods
- Frequency divider
- Examples
- Current research topics

Motivations

Preamble

- Let's consider the two-machine system:

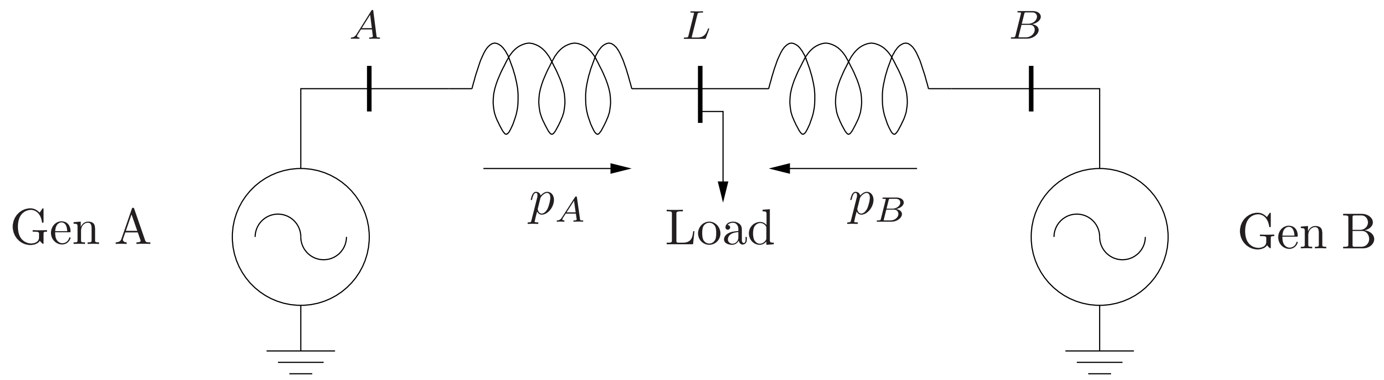

- Conventional Model:

$$\frac{d\delta_A}{dt} = \omega_n(\omega_A - \omega_s) \qquad \frac{d\delta_B}{dt} = \omega_n(\omega_B - \omega_s)$$

$$\frac{d\omega_A}{dt} = \frac{1}{M_A}(p_{mA} - p_A) \qquad \frac{d\omega_B}{dt} = \frac{1}{M_B}(p_{mB} - p_B)$$

$$p_A = \frac{e'_A v_L}{x'_{dA} + x_{\mathrm{AL}}} \sin(\delta_A - \delta_L) \qquad p_B = \frac{e'_B v_L}{x'_{dA} + x_{\mathrm{BL}}} \sin(\delta_B - \delta_L)$$

Turkey Blackout on 31st of March 2015 – I

- The blackout in Turkey led to the outage of 32 GW.

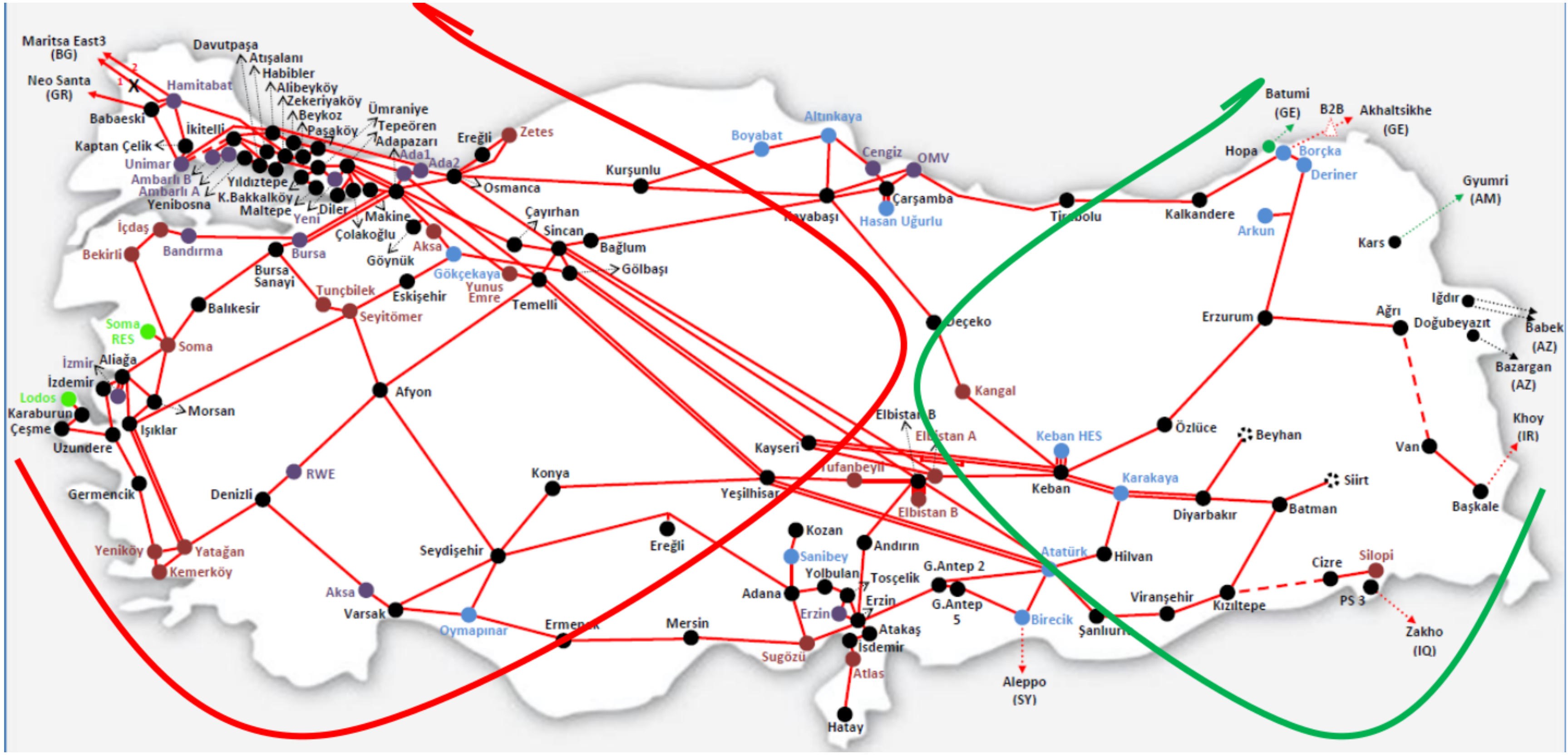

Turkey Blackout on 31st of March 2015 – II

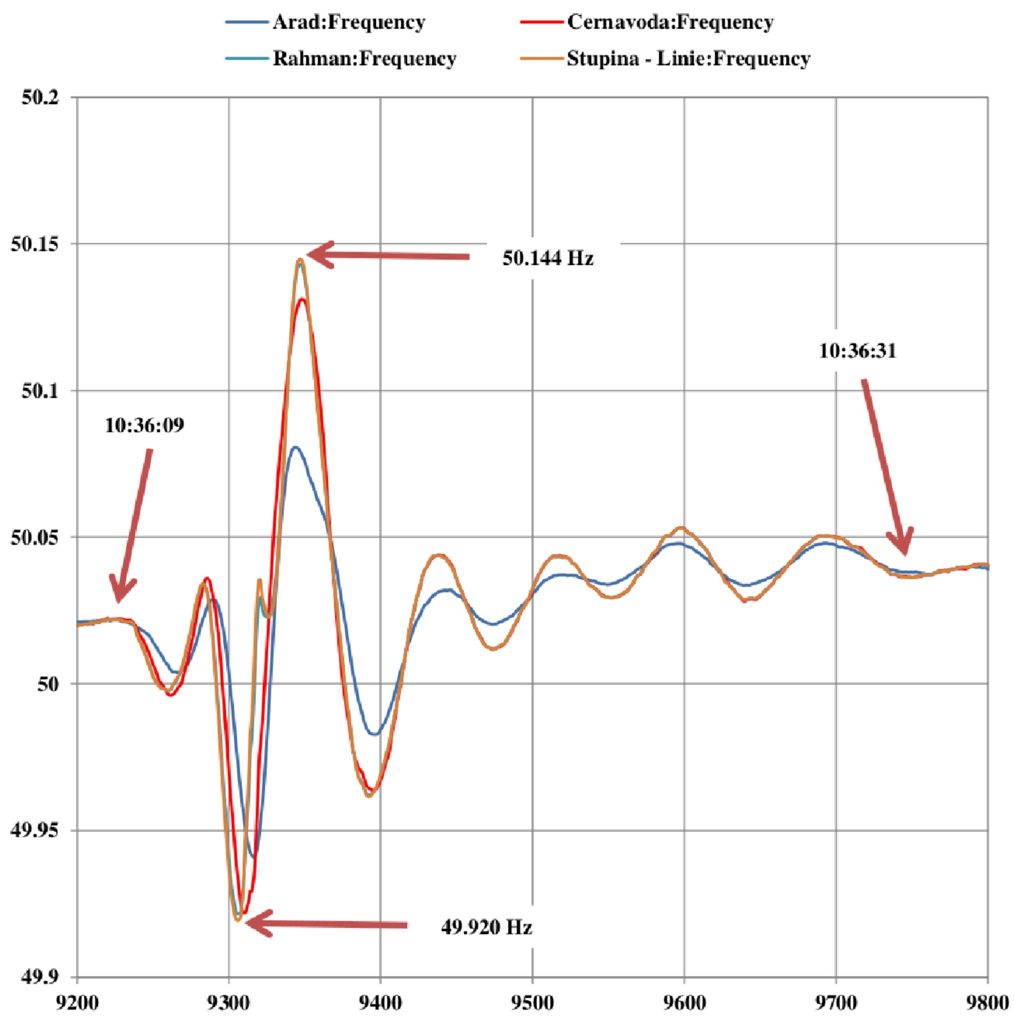

- As a consequence of the line outages and the blackout in Turkey, the Romanian system experimented severe frequency oscillations.
- Bigger oscillations were measured at locations geographically closer to Turkey.

Motivations – I

- The conventional power system model for transient stability analysis is based on the assumption of quasi-steady-state phasors for voltages and currents.
- The crucial hypothesis on which such a model is defined is that the frequency required to define all phasors and system parameters is constant and equal to its nominal value.
- This model is appropriate as long as only the rotor speed variations of synchronous machines is needed to regulate the system frequency through standard primary and secondary frequency regulators.

Motivations – II

- In recent years, however, an increasing number of devices other than synchronous machines are expected to provide frequency regulation.
- These include, among others:
  - distributed energy resources, e.g., wind and solar generation
  - flexible loads providing load demand response
  - HVDC transmission systems
  - energy storage devices
- However, these devices do not impose the frequency at their connection point with the grid.
- There is thus the need to define with accuracy the local frequency at every bus of the network.

Existing Methods

Center of Inertia

- The *center of inertia* (COI) is a weighted arithmetic average of the rotor speeds of synchronous machines that are connected to a transmission system:

$$\omega_{\mathrm{COI}} = \frac{\sum_{j \in \mathcal{G}} H_j \omega_j}{\sum_{j \in \mathcal{G}} H_j}$$

  where ω_j and H_j are the rotor speed and the inertia constant, respectively, of the synchronous machine j and $\mathcal{G}$ is the set of synchronous machines belonging to a given cluster.

Derivative of the Bus Voltage Phase Angle (θ)

- The frequency estimation is obtained by means of a washout and a low-pass filter.
- The washout filter approximates the derivative of the input signal.
- $T_f = 3/\Omega_n$ s and $T_\omega = 0.05$ s are used as default values for all simulations.

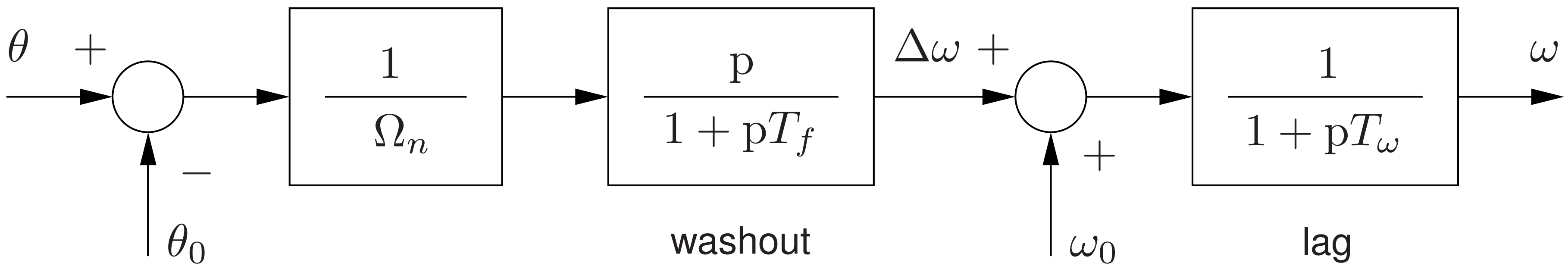

Frequency Divider

Nodal Equations – I

- The very starting point is the augmented admittance matrix, with inclusion of synchronous machine internal impedances as it is commonly defined for fault analysis.
- System currents and voltages are linked as follows:

$$\begin{bmatrix} \bar{\boldsymbol{i}}_G \\ \bar{\boldsymbol{i}}_B \end{bmatrix} = \begin{bmatrix} \bar{\mathbf{Y}}_{GG} & \bar{\mathbf{Y}}_{GB} \\ \bar{\mathbf{Y}}_{BG} & \bar{\mathbf{Y}}_{BB} + \bar{\mathbf{Y}}_{B0} \end{bmatrix} \begin{bmatrix} \bar{\boldsymbol{e}}_G \\ \bar{\boldsymbol{v}}_B \end{bmatrix} \tag{1}$$

where $\bar{\boldsymbol{v}}_B$ and $\bar{\boldsymbol{i}}_B$ are bus voltages and current injections, respectively, at network buses; $\bar{\boldsymbol{i}}_G$ are generator current injections; $\boldsymbol{e}_G$ are generator emfs behind the internal generator impedance; $\bar{\mathbf{Y}}_{BB}$ is the standard network admittance matrix; $\bar{\mathbf{Y}}_{GG}$, $\bar{\mathbf{Y}}_{GB}$ and $\bar{\mathbf{Y}}_{BG}$ are admittance matrices obtained using the internal impedances of the synchronous machines; and $\bar{\mathbf{Y}}_{B0}$ is a diagonal matrix that accounts for the internal impedances of the synchronous machines at generator buses.

Nodal Equations – II

- All quantities in (1) depend on the frequency.
- However, the dependency of the admittance matrices above on the frequency is neglected.
- This approximation has a small impact on the accuracy of the frequency estimation and allows determining a compact expression of bus frequencies, as discussed in the remainder of this section.

Nodal Equations – III

- To further elaborate on (1), let us assume that load current injections $\bar{\boldsymbol{i}}_B$ can be neglected in (1).
- This is justified by the fact that the equivalent load admittance, in trasmission systems, is typically one order of magnitude smaller than that of the diagonal elements of $\bar{\mathbf{Y}}_{BB} + \bar{\mathbf{Y}}_{B0}$.
- This appears as a critical assumption, and for this reason we test its adequateness in the examples, where we'll consider a variety of load models, including nonlinear dynamic ones.

Nodal Equations – IV

- Let's rewrite (1) as follows:

$$\begin{bmatrix} \bar{\boldsymbol{i}}_G \\ \mathbf{0} \end{bmatrix} = \begin{bmatrix} \bar{\mathbf{Y}}_{GG} & \bar{\mathbf{Y}}_{GB} \\ \bar{\mathbf{Y}}_{BG} & \bar{\mathbf{Y}}_{BB} + \bar{\mathbf{Y}}_{B0} \end{bmatrix} \begin{bmatrix} \bar{\boldsymbol{e}}_G \\ \bar{\boldsymbol{v}}_B \end{bmatrix} \tag{2}$$

- Bus voltages $\bar{\boldsymbol{v}}_B$ are thus a function of generator emfs and can be computed explicitly:

$$\begin{aligned} \bar{\boldsymbol{v}}_B &= -[\bar{\mathbf{Y}}_{BB} + \bar{\mathbf{Y}}_{B0}]^{-1} \bar{\mathbf{Y}}_{BG} \bar{\boldsymbol{e}}_G \\ &= \bar{\mathbf{D}}\, \bar{\boldsymbol{e}}_G \end{aligned} \tag{3}$$

Time Derivative in the dq-frame – I

- Let's consider the time derivative – indicated with the functional $\mathrm{p}(\cdot)$ – of the bus voltage phasors in a dq-frame rotating with frequency ω_0:

$$\mathrm{p}\bar{v}_{\mathrm{dq},h} = \frac{d}{dt}\bar{v}_{\mathrm{dq},h} + j\omega_0\bar{v}_{\mathrm{dq},h} \quad (4)$$

  where $\bar{v}_{\mathrm{dq},h} = v_{\mathrm{d},h} + jv_{\mathrm{q},h}$.

- A similar expression can be also obtained using a first order dynamic phasor approximation.

Time Derivative in the dq-frame – II

- The first element on the right-hand side of (4) is the time derivative of $\bar{v}_{\mathrm{dq},h}$, which is rotating with the dq-frame, while the second element is the derivative of the dq-frame itself.

- We now assume the following:
  - The quasi-steady-state phasor can be approximated, during an electromechanical transient, to the dq-frame quantity, hence:

$$\bar{v}_h \approx \bar{v}_{\mathrm{dq},h} \tag{5}$$

    Note that in stationary conditions the equality $\bar{v}_h = \bar{v}_{\mathrm{dq},h}$ holds.
  - The voltage is a sinusoid with time-varying pulsation and its time derivative in (4) is approximated with:

$$\frac{d}{dt}\bar{v}_{\mathrm{dq},h} \approx j\Delta\omega_h \bar{v}_{\mathrm{dq},h} \tag{6}$$

    where $\Delta\omega_h$ is the frequency deviation with respect to ω_0 at bus h.

Time Derivative in the dq-frame – III

- Equation (6) descends from the hypothesis of assuming “slow” variations of the frequency in the system and is consistent with the standard electromechanical power system model utilized for transient stability analysis.
- Merging together (4), (5) and (6) leads to:

$$\mathrm{p}\,\bar{v}_h \approx j\,\omega_h\,\bar{v}_h \tag{7}$$

where $\omega_h = \omega_0 + \Delta\omega_h$ is the frequency at bus h.

- Expressions similar to (7) hold for all other ac quantities in the systems, i.e., generator emfs $\bar{e}$ and currents.
- For example:

$$\mathrm{p}\,\bar{e}_i \approx j\,\omega_i\,\bar{e}_i \tag{8}$$

where ω_i is the rotor speed of generator i.

Merging Nodal Equations and dq-frame – I

- We now use the approximated time derivatives (7) and (8) along with network constraints (3) to determine the frequency divider.
- Differentiating (3) with respect to time leads to:

$$\mathrm{p}\bar{\boldsymbol{v}}_B = \mathrm{p}[\bar{\mathbf{D}} \cdot \bar{\boldsymbol{e}}_G] = \mathrm{p}\bar{\mathbf{D}} \cdot \bar{\boldsymbol{e}}_G + \bar{\mathbf{D}} \cdot \mathrm{p}\bar{\boldsymbol{e}}_G \tag{9}$$

$$\Rightarrow \quad \mathrm{p}\bar{\boldsymbol{v}}_B \approx \bar{\mathbf{D}} \cdot \mathrm{p}\bar{\boldsymbol{e}}_G \tag{10}$$

$$\Rightarrow \quad \frac{d}{dt}\bar{\boldsymbol{v}}_B + j\omega_0\bar{\boldsymbol{v}}_B \approx \bar{\mathbf{D}} \cdot \frac{d}{dt}\bar{\boldsymbol{e}}_G + j\omega_0\bar{\mathbf{D}} \cdot \bar{\boldsymbol{e}}_G \tag{11}$$

$$\Rightarrow \quad j\,\mathrm{diag}(\Delta\boldsymbol{\omega}_B)\,\bar{\boldsymbol{v}}_B \approx j\,\bar{\mathbf{D}} \cdot \mathrm{diag}(\Delta\boldsymbol{\omega}_G)\,\bar{\boldsymbol{e}}_G \tag{12}$$

Merging Nodal Equations and dq-frame – II

- More assumptions are needed to obtain (9), as follows:
  - in (9), it is assumed that $\mathrm{p}\bar{\mathbf{D}} \approx \mathbf{0}$, i.e., constant transmission line, transformer, load and generator parameters;
  - in (10), the time derivative $\mathrm{p}(\cdot)$ is expanded using (4);
  - in (11), (3) is utilized to eliminate the terms $j\omega_0 \bar{\boldsymbol{v}}_B$ and $j\omega_0 \bar{\mathbf{D}} \cdot \bar{\boldsymbol{e}}_G$; and
  - $\mathrm{diag}(\cdot)$ indicates a matrix where diagonal elements are the elements of its argument vector.

Merging Nodal Equations and dq-frame – III

- Based on (6), (7) and (8), $\Delta\boldsymbol{\omega}_B$ and $\Delta\boldsymbol{\omega}_G$ are:

$$\begin{aligned} \Delta\boldsymbol{\omega}_B &= \boldsymbol{\omega}_B - \omega_0 \cdot \mathbf{1} \\ \Delta\boldsymbol{\omega}_G &= \boldsymbol{\omega}_G - \omega_0 \cdot \mathbf{1} \end{aligned} \tag{13}$$

- The set of equations (12) and (13) allows determining the bus voltage frequencies $\boldsymbol{\omega}_B$.
- In fact, $\bar{\mathbf{D}}$ are parameters and $\boldsymbol{\omega}_G$, $\bar{\boldsymbol{v}}_B$ and $\bar{\boldsymbol{e}}_G$ are variables determined by integrating the set of DAEs describing the power system.
- While solvable, (12) can be significantly simplified without a relevant loss of accuracy.

Merging Nodal Equations and dq-frame – IV

- The following approximations and assumptions are applied:
  - $\bar{\boldsymbol{v}}_B \approx \mathbf{1}$ pu and $\bar{\boldsymbol{e}}_G \approx \mathbf{1}$ pu;
  - The conductances of the elements of all admittance matrices utilized to compute $\bar{\mathbf{D}}$ are negligible, e.g., $\bar{\mathbf{Y}}_{BB} \approx j\mathbf{B}_{BB}$;
  - The condition $\omega_0 = 1$ pu usually holds.

Frequency Divider Formula

- Finally, substituting frequency deviations with the expressions in (13), (12) leads to **the proposed frequency divider formula**:

$$\boxed{\boldsymbol{\omega}_B = \mathbf{1} + \mathbf{D}(\boldsymbol{\omega}_G - \mathbf{1})} \tag{14}$$

where

$$\mathbf{D} = -(\mathbf{B}_{BB} + \mathbf{B}_{B0})^{-1}\mathbf{B}_{BG} \tag{15}$$

- The formula has the same formal structure of voltage dividers in resitive dc circuits.

Inclusion of Frequency Measurements – I

- The frequency divider formula can be modified to include frequency measurements as provided, for example, by PMU devices, as follows.
- Let's assume that, apart from synchronous machine rotor speeds, also the bus voltage phasors $\bar{\boldsymbol{v}}_M$ and hence bus frequencies $\boldsymbol{\omega}_M$ are known at a given set of network buses.
- Such frequencies can be used to compute the remaining unknown bus frequencies.
- Say that $\boldsymbol{\omega}_B = [\boldsymbol{\omega}_M, \boldsymbol{\omega}_U]$, where $\boldsymbol{\omega}_U$ are the remaining unknown bus frequencies.

Inclusion of Frequency Measurements – II

- Using same notation as for (1), one has:

$$\begin{bmatrix} \bar{\boldsymbol{i}}_G \\ \bar{\boldsymbol{i}}_M \\ \bar{\boldsymbol{i}}_B \end{bmatrix} = \begin{bmatrix} \bar{\mathbf{Y}}_{GG} & \bar{\mathbf{Y}}_{GM} & \bar{\mathbf{Y}}_{GU} \\ \bar{\mathbf{Y}}_{MG} & \bar{\mathbf{Y}}_{MM} + \bar{\mathbf{Y}}_{M0} & \bar{\mathbf{Y}}_{MU} \\ \bar{\mathbf{Y}}_{UG} & \bar{\mathbf{Y}}_{UM} & \bar{\mathbf{Y}}_{UU} + \bar{\mathbf{Y}}_{U0} \end{bmatrix} \begin{bmatrix} \bar{\boldsymbol{e}}_G \\ \bar{\boldsymbol{v}}_M \\ \bar{\boldsymbol{v}}_B \end{bmatrix} \tag{16}$$

- Following the same derivations discussed above, the frequency divider formula (14) becomes:

$$\boldsymbol{\omega}_U = -(\mathbf{B}_{UU} + \mathbf{B}_{U0})^{-1} \begin{bmatrix} \mathbf{B}_{UG} & \mathbf{B}_{UM} \end{bmatrix} \begin{bmatrix} \boldsymbol{\omega}_G \\ \boldsymbol{\omega}_M \end{bmatrix} \tag{17}$$

Inclusion of Frequency Measurements – III

- The expression above can be used in two ways.
  - In simulations, one can model PMU devices and use their measures to obtain a better estimation of the frequencies at remaining buses.
  - In state-estimation, using real-world frequency measures obtained from the system to estimate frequency variations at remaning system buses.

Examples

Radial System – I

- Let assume a lossless connection, with total reactance $x_{hk} = x_{hi} + x_{ik}$.
- The frequencies at buses h and k, say ω_h and ω_k, respectively, are the rotor speeds of the synchronous generators.

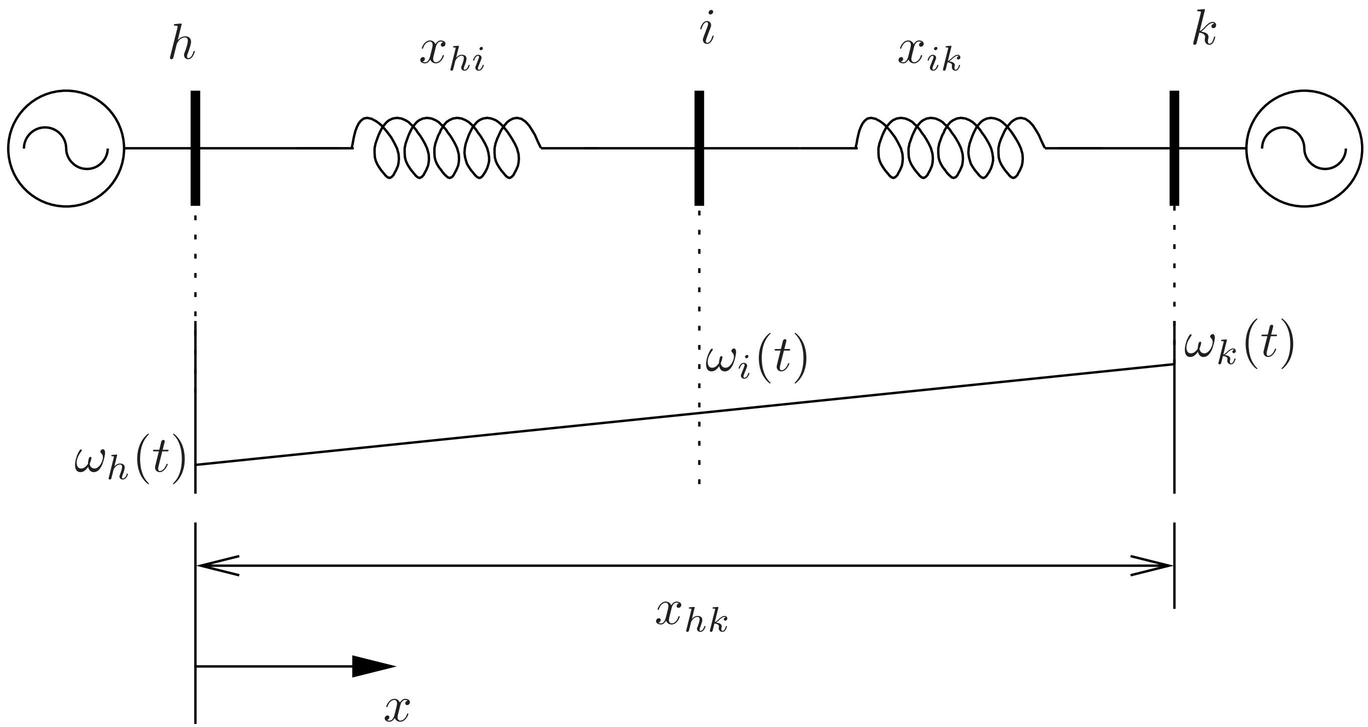

Radial System – II

- Applying the frequency divider formula (14), we obtain:

$$
\begin{aligned}
\omega_i(t) = \boldsymbol{D} \cdot \begin{bmatrix} \omega_h(t) \\ \omega_k(t) \end{bmatrix} &= -(\boldsymbol{B}_{BB} + \boldsymbol{B}_{B0})^{-1} \boldsymbol{B}_{BG} \cdot \begin{bmatrix} \omega_h(t) \\ \omega_k(t) \end{bmatrix} \\
&= \left[\frac{1}{x_{hi}} + \frac{1}{x_{ik}}\right]^{-1} \begin{bmatrix} \dfrac{1}{x_{hi}} & \dfrac{1}{x_{ki}} \end{bmatrix} \cdot \begin{bmatrix} \omega_h(t) \\ \omega_k(t) \end{bmatrix} \qquad (18) \\
&= \frac{x_{ik}}{x_{hk}} \cdot \omega_h(t) + \frac{x_{hi}}{x_{hk}} \cdot \omega_k(t)
\end{aligned}
$$

- The instantaneous frequency $\omega_i(t)$ at a generic point i between the boundaries h and k is a linear interpolation between $\omega_h(t)$ and $\omega_k(t)$.

Example – I

- Let's first consider a standard model for transient stability analysis where transmission lines are lumped and modeled as constant impedances and generator flux dynamics are neglected.
- Generators are equal and are modeled as a 6th order synchronous machine with AVRs and turbine governors.
- The load is modeled as a constant admittance. The disturbance is a three-phase fault that occurs at bus 3 at $t = 1$ s and is cleared after 150 ms by opening one of the two lines connecting buses 1 and 3.

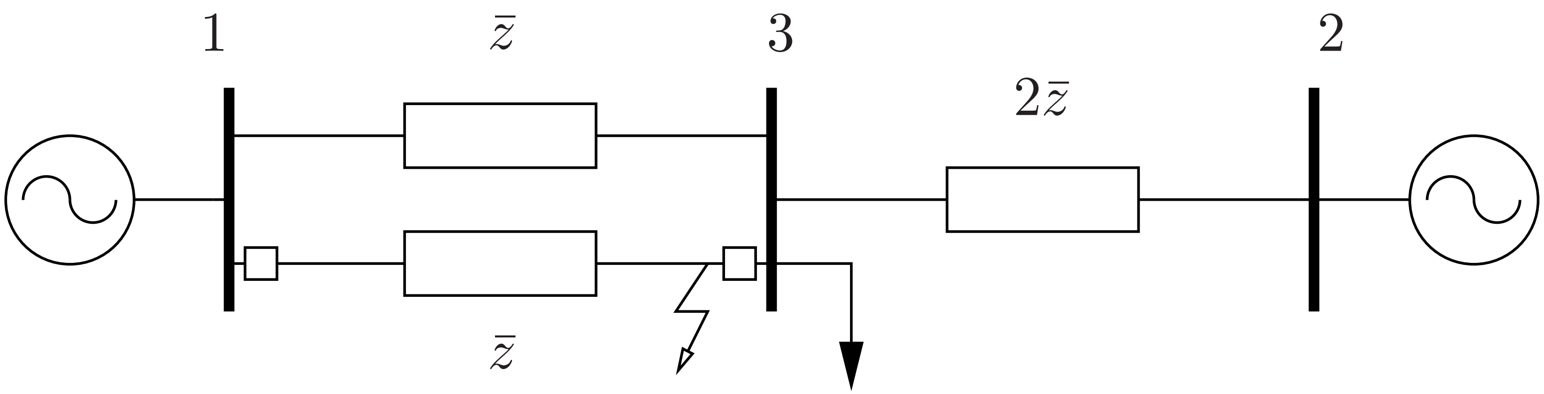

Example – II

- Transient behavior of synchronous machine rotor speeds, the frequency of the COI (ω_{COI}), and the estimated frequency at the load bus using the proposed frequency divider approach.

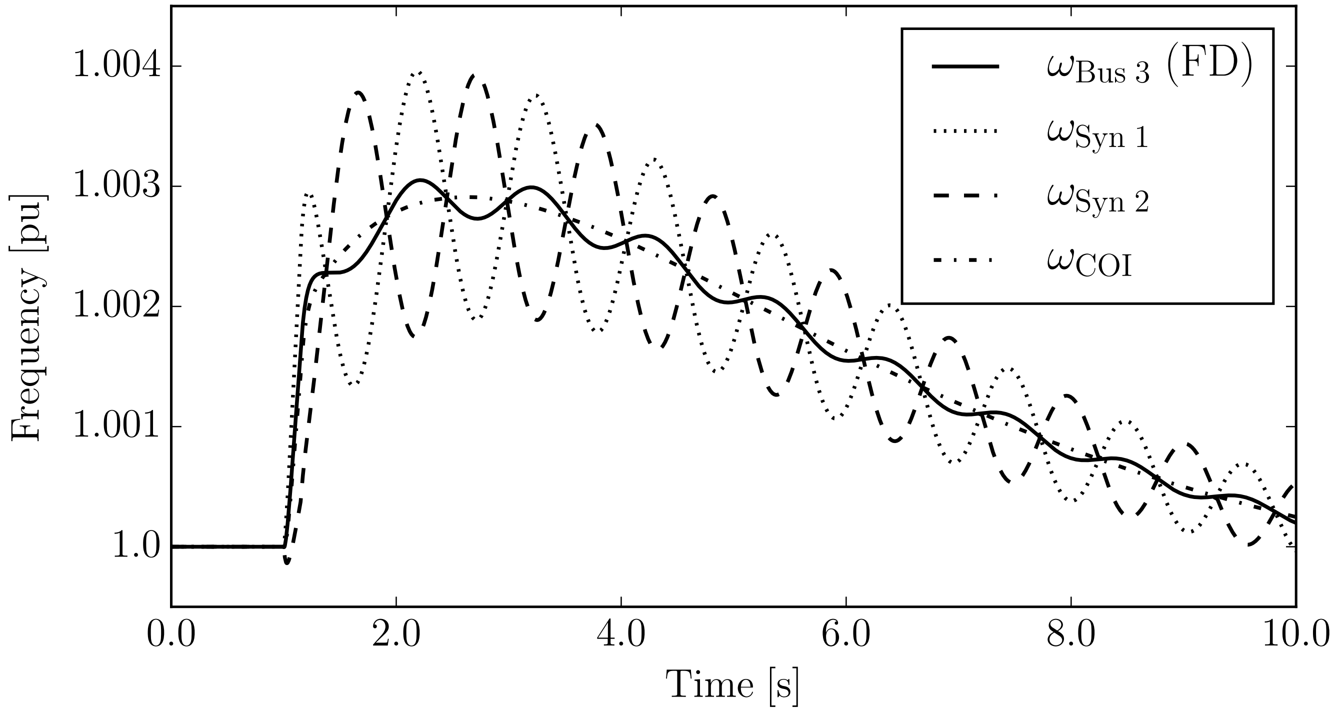

Example – III

- Frequency at bus 3 estimated with the frequency divider (FD) and the conventional washout filter (WF). The system is simulated using the fully-fledged dq-axis model.

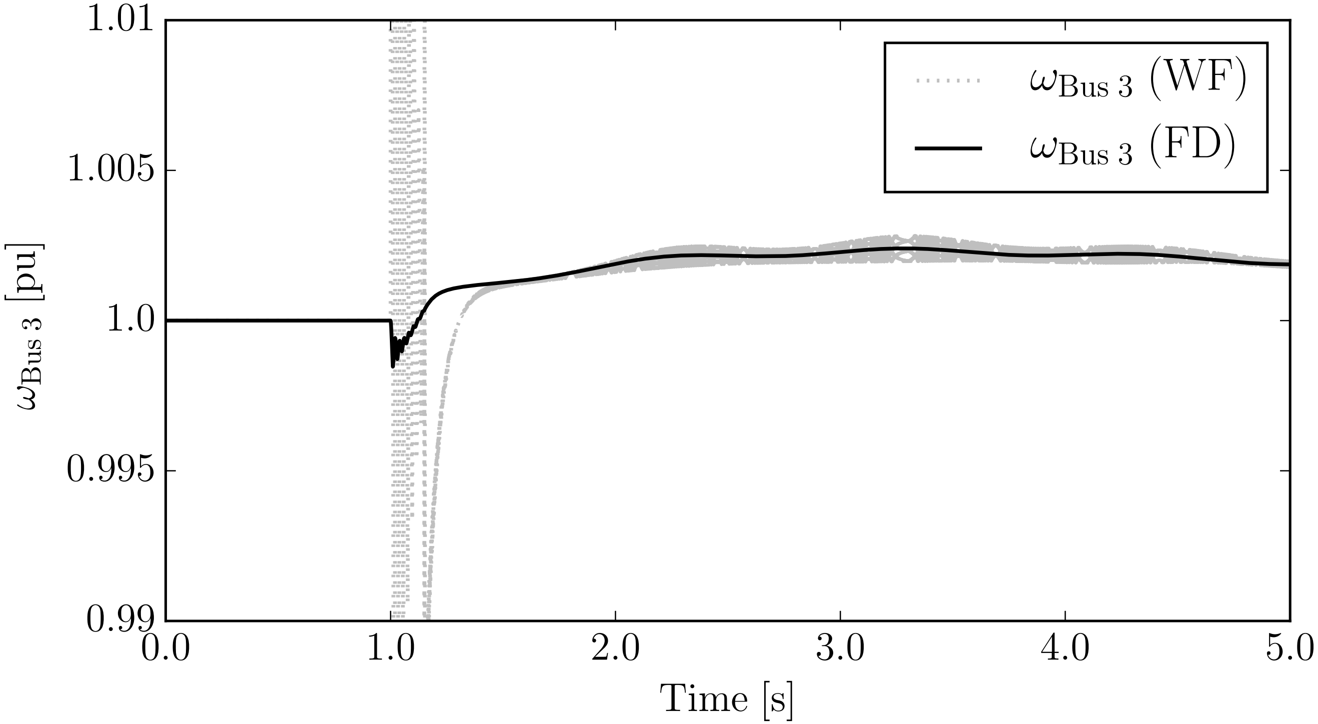

Example – IV

- Frequency at bus 3 estimated with the frequency divider (FD) and the conventional washout filter (WF). The load is modelled as a frequency-dependent load representing an aluminum plant

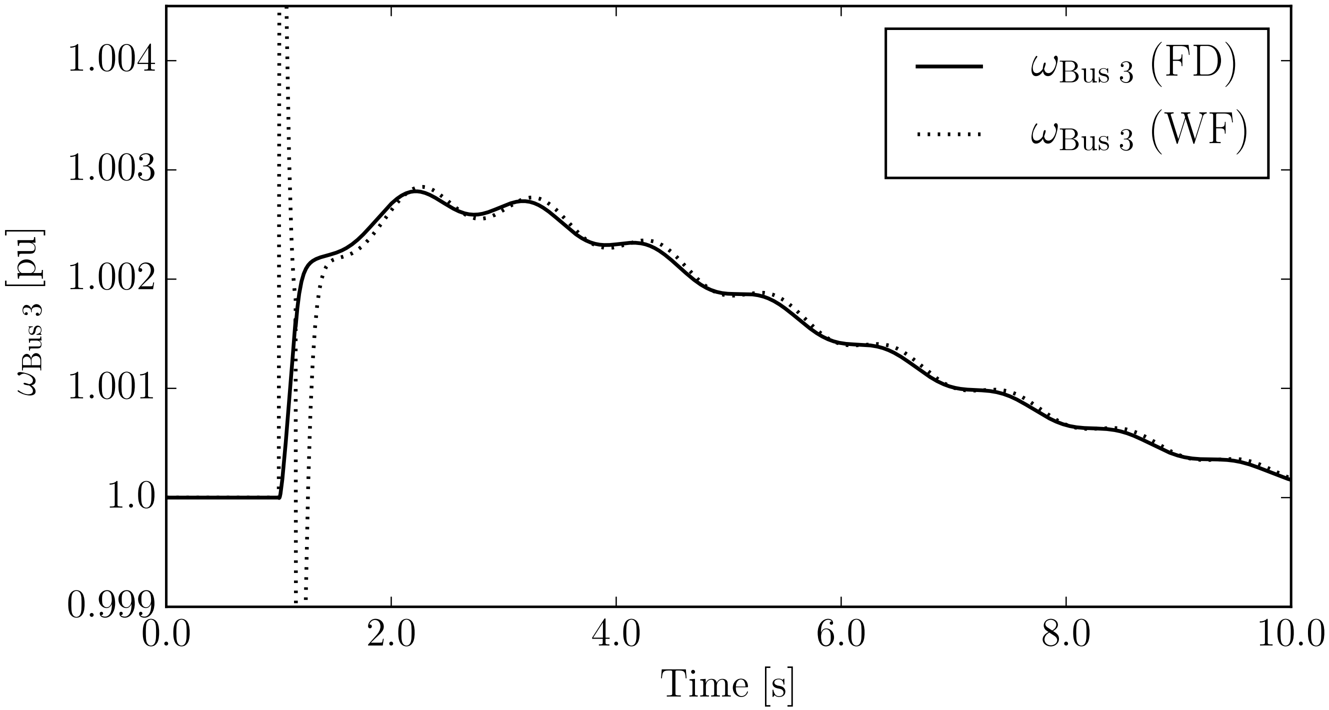

Example – V

- Frequency at bus 3 estimated with the frequency divider (FD) and the conventional washout filter (WF). The load is a squirrel cage induction motor with a 5th-order dq-axis model.

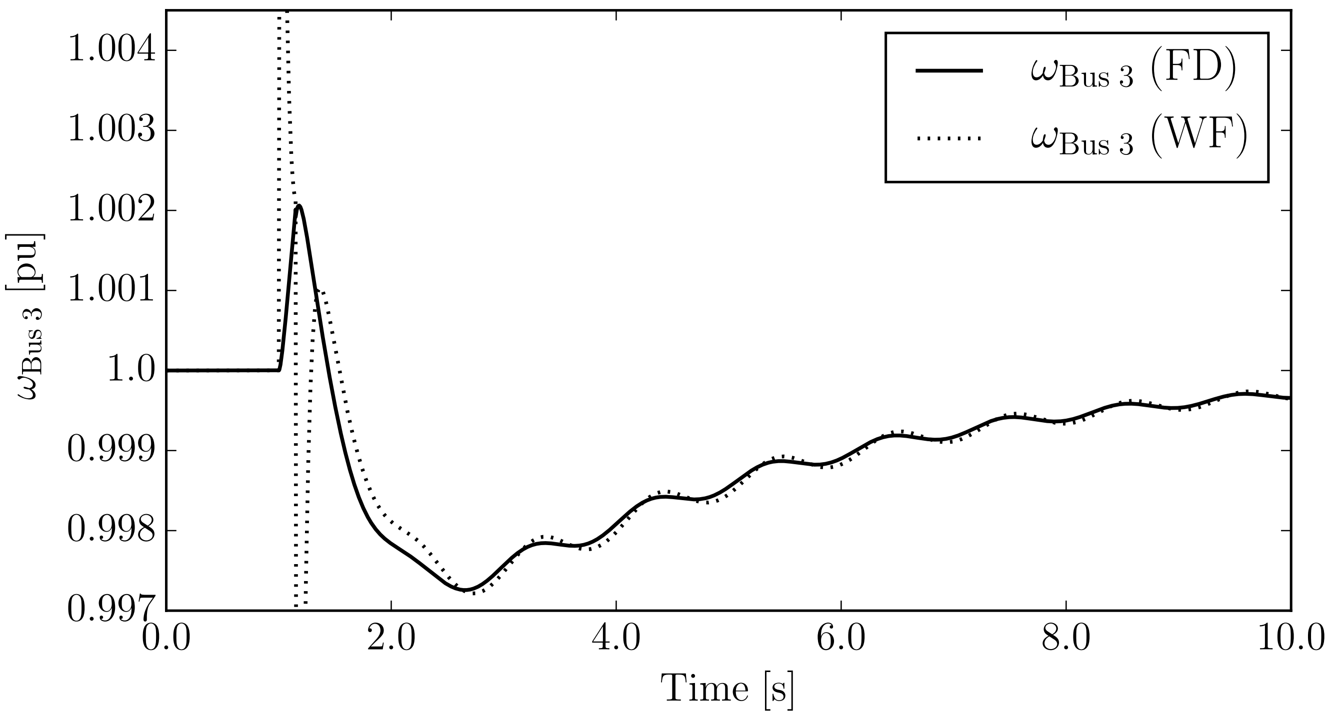

Irish Transmission System – I

- This system includes 1,479 buses, 1,851 transmission lines and transformers, 245 loads, 22 conventional synchronous power plants modeled with 6^{th} order synchronous machine models with AVRs and turbine governors, 6 PSSs and 176 wind power plants, of which 34 are equipped with constant-speed (CSWT) and 142 with doubly-fed induction generators (DFIG).
- The large number of non-conventional generators based on induction machines and power electronics converters makes this system an excellent test-bed to check the accuracy of the proposed frequency divider.

Irish Transmission System – II

- Fault close to a synchronous machine and a load. Frequency at the generator bus.

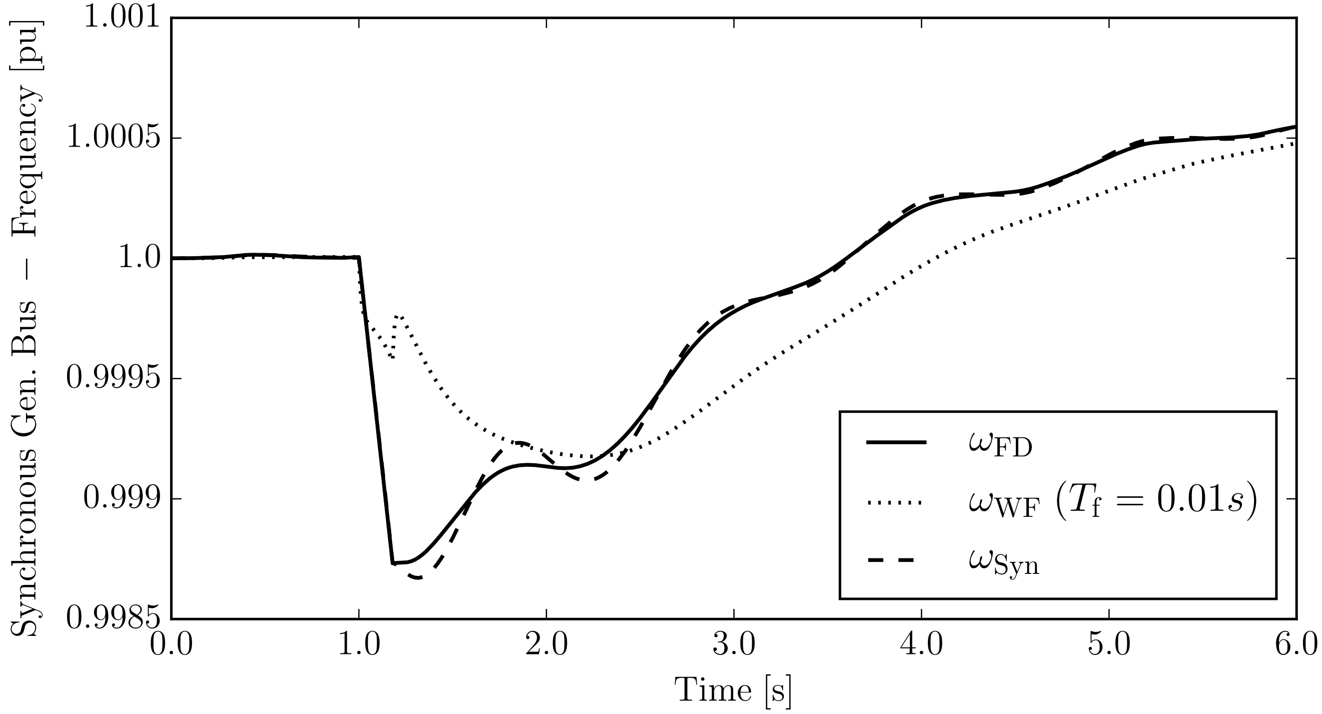

Irish Transmission System – III

- Fault close to a synchronous machine and a load. Frequency at the load bus.

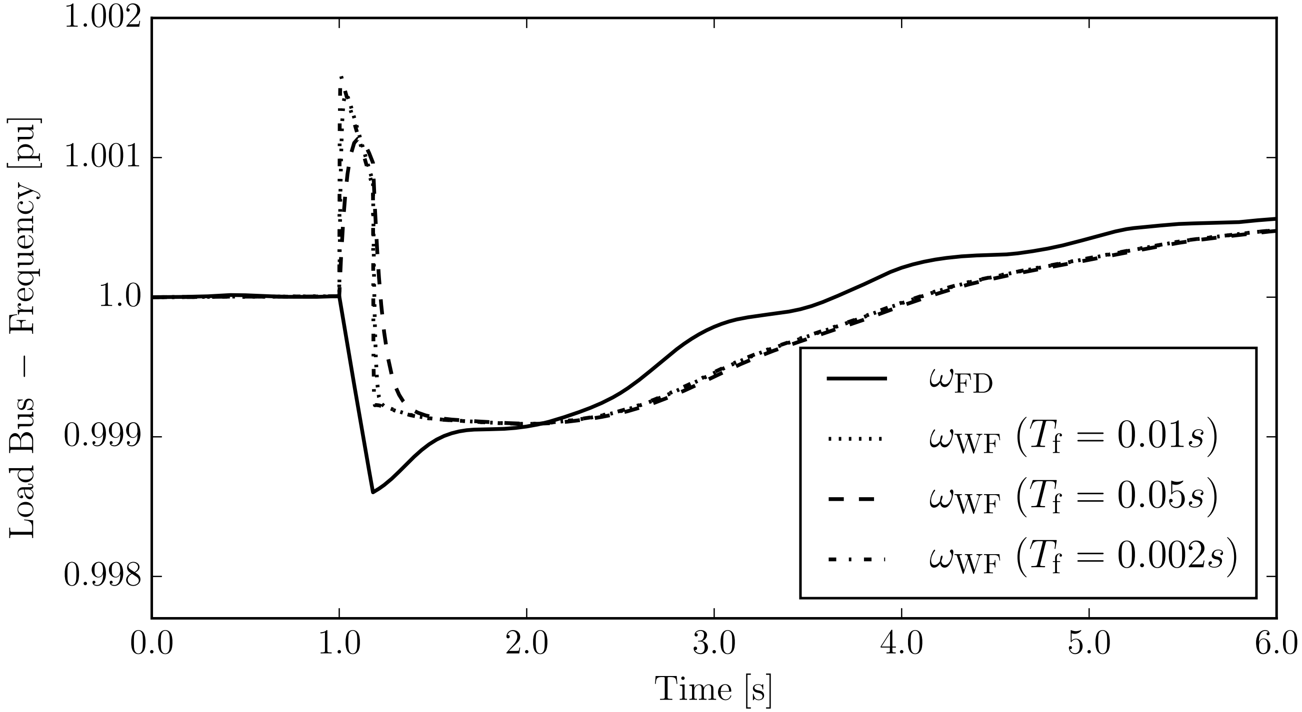

Irish Transmission System – IV

- Frequency response of the Irish transmission system facing a three-phase fault close to a wind power plant.

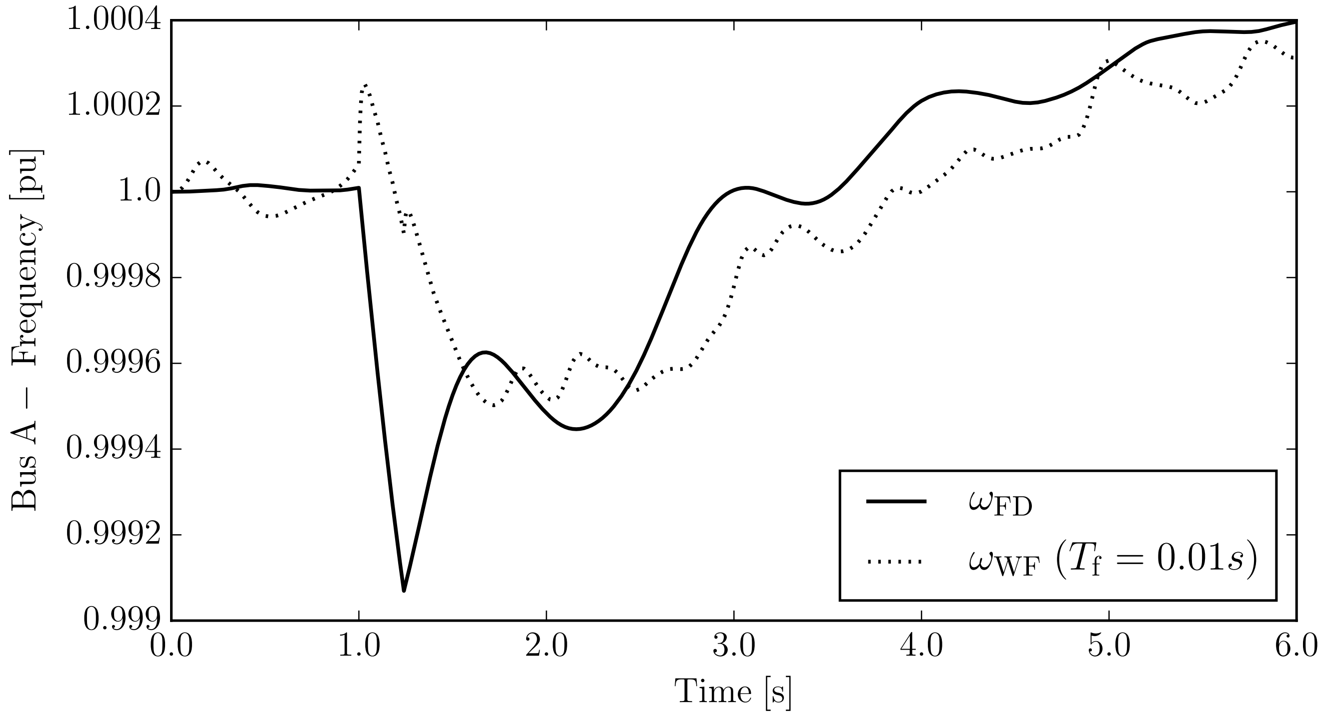

New England 39-bus, 10-machine System – I

- This benchmark network contains 19 loads totaling $7,316.5$ MW and $1,690.9$ MVAr of active and reactive power, respectively (20% load increase with respect to the base case is assumed).
- The system model also includes generator controllers such as primary voltage regulators, as well as both primary and secondary frequency regulation (turbine governors and AGC).
- The system includes also thermostatically controlled loads, which are the 20% of the total load.
- The contingency is a three-phase fault at bus 21, cleared by the opening of the line connecting buses 16 and 21 after 160 ms.

New England 39-bus, 10-machine System – II

- Rotor speed of the synchronous generator in bus 31 (Gen 2) using 3^{rd} order synchronous machine models.

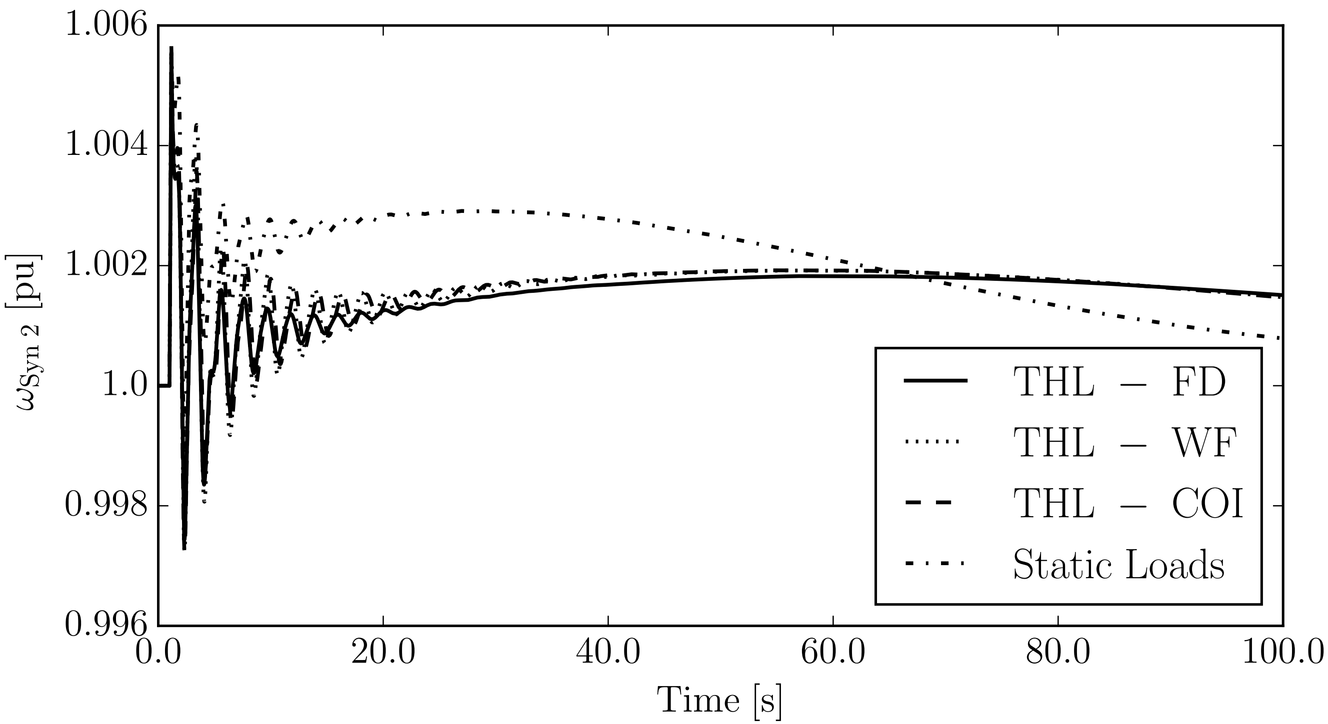

New England 39-bus, 10-machine System – III

- Rotor speed of the synchronous generator in bus 31 (Gen 2) using 6^{th} order synchronous machine models.

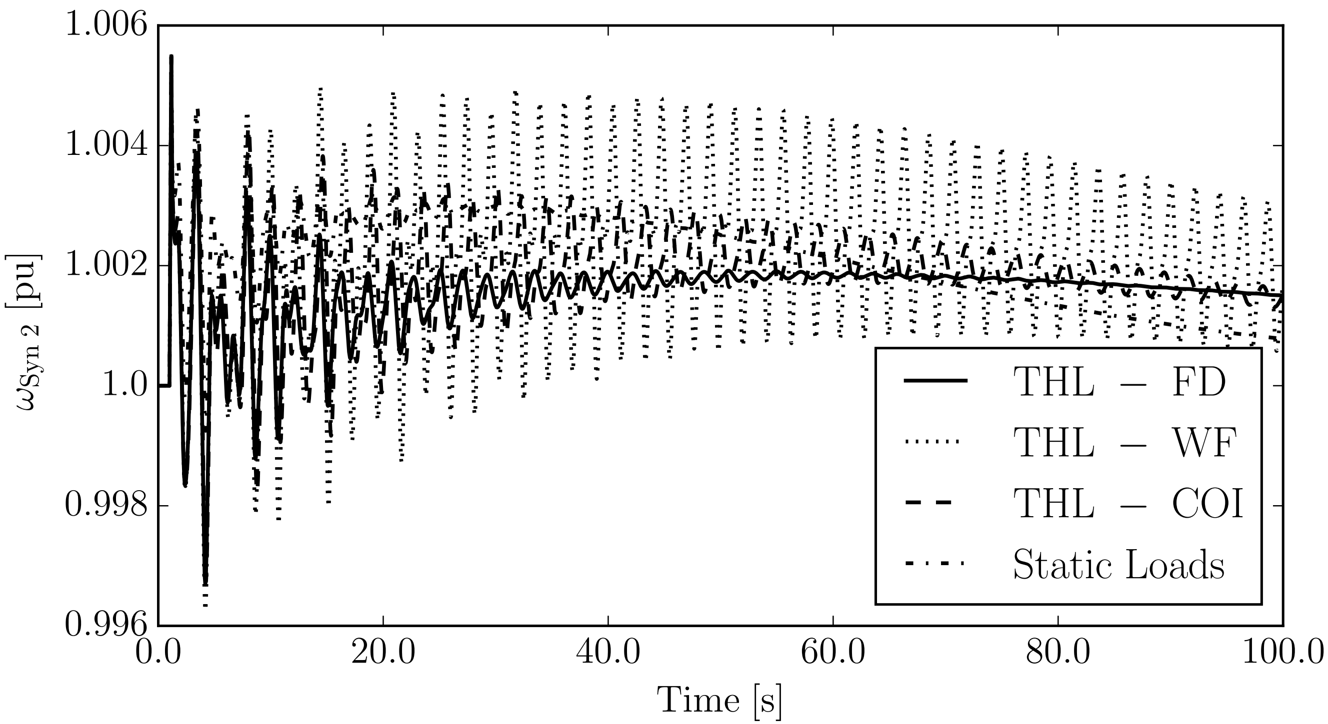

New England 39-bus, 10-machine System – IV

- Rotor speed of the synchronous generator in bus 31 (Gen 2) using 8^{th} order synchronous machine models.

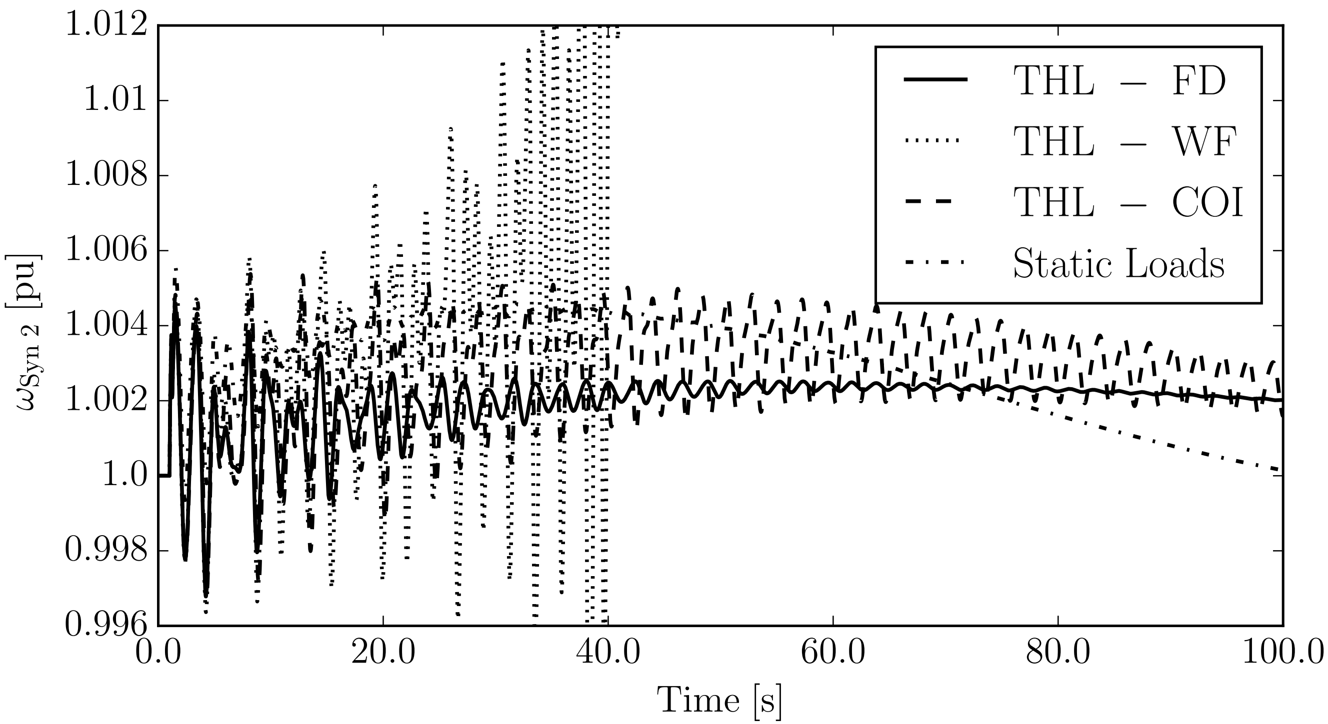

ENTSO-E Transmission System – I

- The model includes 21,177 buses (1,212 off-line); 30,968 transmission lines and transformers (2,352 off-line); 1,144 coupling devices, i.e., zero-impedance connections (420 off-line); 15,756 loads (364 off-line); and 4,828 power plants.
- Of these power plants, 1,160 power plants are off-line. The system also includes 364 PSSs.

ENTSO-E Transmission System – II

- Size and number of non-zeros (NNZ) elements of matrices $\mathbf{B}_{BB}$, $\mathbf{B}_{G0}$, $\mathbf{B}_{BG}$ and $\mathbf{D}$ for the ENTSO-E system.

Matrix	Size	NNZ	NNZ $\%$
$\mathbf{B}_{BB}$	$21,177 \times 21,177$	$72,313$	0.0161
$\mathbf{B}_{BG}$	$21,177 \times 4,832$	$4,832$	0.0047
$\mathbf{B}_{G0}$	$21,177 \times 21,177$	$3,245$	0.0007
$\mathbf{B}_{BB} + \mathbf{B}_{G0}$	$21,177 \times 21,177$	$72,313$	0.0161
$\mathbf{D}$	$21,177 \times 4,832$	$86,169,456$	84.2

ENTSO-E Transmission System – III

- The inverse of a sparse matrix can be very dense ...
- ... and trying to actually compute $\mathbf{D}$ leads to memory overflow for the ENTSO-E system!
- Hence, the most efficient implementation of the freqeuncy divider formula is the following *acausal* expression:

$$\mathbf{0} = (\mathbf{B}_{BB} + \mathbf{B}_{G0}) \cdot (\boldsymbol{\omega}_B - \mathbf{1}) + \mathbf{B}_{BG} \cdot (\boldsymbol{\omega}_G - \mathbf{1})$$

Conclusions, Future Work

and References

Conclusions (for now . . .)

- A general expression to estimate frequency variations during the transient of electric power systems has been deduced.
- The proposed expression is derived based on standard assumptions of power system models for transient stability analysis and can be readily implemented in power system software tools for transient stability analysis.
- The formula is aimed at improving the accuracy of bus frequency estimation in traditional electromechanical power system models.
- Simulation results show that the proposed formula is accurate, numerically robust and computationally efficient.

Open Challenges

- How to take into account fast flux transients?
- How to couple the proposed frequency divider with the effect of the frequency controllers of non-synchronous devices, such as distributed generation and flexible loads?
- What if there are **no** synchronous machines?
- Thorough testing is required . . .
- PMU measurements are needed!

References

- F. Milano, Á. Ortega, *Frequency Divider*, IEEE Transactions on Power Systems, accepted on May 2016, in press.
- Á. Ortega, F. Milano, *Comparison of Bus Frequency Estimators for Power System Transient Stability Analysis*, IEEE PowerCon, Wollongong, Australia, September 28th – October 1st, 2016.

Horizon 2020 Project

- RE-SERVE – *Renewables in a Stable Electric Grid*
- 3 years, started on the 1st of October, 2016
- Work Package 2 (leader UCD): Frequency stability analysis
  - Novel frequency controls based on non-synchronous generation
  - Modelling freqeuncy variations in transient stbaility models
  - Angle and frequency stability for system with low inertia
  - 5G telecommincation technology
  - Recommendation to ISOs re frequency regulation

Current Research Topics

My Current Research Topics

- Power system modelling:
  - Stochastic differential equations (e.g., impact of uncertainty and volatility)
  - Functional differential equations (e.g., control signal delay)
  - Hybrid differential equations (e.g., digital/continuous signals, discontinuities)
  - (Semi-)Implicit formulation of differential-algebraic equations
  - Parallelization and HPC
- Power system stability and control (e.g., bifurcation theory, Lyapunov methods/exponents, homotopy theory, etc.)
- Power system optimization (nonlinear programming, OPF, MPC)

Thanks much for your attention!